

# ON MAGNETOHYDRODYNAMIC INSTABILITIES AT VENUS

H. K. Biernat<sup>1 2</sup>  
N. V. Erkaev<sup>3</sup>  
I. L. Arshukova<sup>3</sup>  
T. Penz<sup>1</sup>  
U. V. Amerstorfer<sup>1</sup>

## Abstract

A magnetohydrodynamic (MHD) model describing the solar wind past Venus is used to study the plasma behavior in the magnetosheath. It is shown that the largest flow velocities are found at the equatorial flanks, while the largest plasma density is found near the subsolar point. The results of the model are used to study the stability of the Venusian ionopause against MHD instabilities. We show that both, the interchange and the Kelvin–Helmholtz instability, have growth times smaller than the magnetic barrier formation time. This indicates that these instabilities can evolve into a nonlinear stage, which can lead to the detachment of plasma clouds from the Venusian ionosphere.

## 1 Introduction

We review a model of the magnetohydrodynamic solar wind flow past Venus using so-called magnetic string equations (Biernat et al., 1999), which we have used successfully in terrestrial and planetary applications (Farrugia et al., 1995; Erkaev et al., 1996). Within this approach, which is partly analytical and partly numerical, we are able to consider the influence of the magnetic field on the plasma flow from the beginning, including the region of the magnetic barrier, where the magnetic pressure exceeds the plasma pressure. We make the main assumption that the variation of the sum of the gas and thermal pressures along a given normal to the ionopause is prescribed. Even though Venus is unmagnetized, the flow of the solar wind is strongly affected by the interplanetary magnetic field (IMF). This effect becomes stronger as the ionopause is approached (Bauer, 1973), leading to the formation of the magnetic barrier. The effect also intensifies, when the Alfvén Mach number upstream of the bow shock decreases.

The solar wind flow around Venus is a background for charge exchange processes and also for instabilities providing momentum and mass exchange between the solar wind and exosphere plasmas in the vicinity of the ionopause. Including pick-up processes, we study the contribution to the structure of the Venus magnetosheath made by pick-up ions

---

<sup>1</sup>Space Research Institute, Austrian Academy of Sciences, Schmiedlstrasse 6, A-8042 Graz, Austria

<sup>2</sup>Institute of Physics, University of Graz, Universitätsplatz 5, A-8010 Graz, Austria

<sup>3</sup>Institute for Computational Modelling, Russian Academy of Sciences, 660036 Krasnoyarsk 36, Russian Federation

(Biernat et al., 2001). The mass loading term (Kallio et al., 1998) is incorporated as a source term in the equation of mass continuity in order to keep the one-fluid nature of the model. This model is suited to study the structure of depletion layers in general, and the magnetic barrier of Venus in particular.

A special feature of the interaction between the solar wind and the ionosphere of Venus is the occurrence of magnetohydrodynamic (MHD) instabilities. The first observational evidence for wavelike plasma irregularities, observed at the top of the dayside ionosphere, and plasma clouds, observed above the ionopause primarily near the terminator and further downstream, were made by the Pioneer Venus Orbiter (PVO). The detailed analysis of several plasma clouds has shown that the plasma within the clouds themselves is ionosphere-like in electron temperature and density (Brace et al., 1982). When such plasma clouds were seen far above the ionosphere, they were clearly separated by an intervening region of magnetosheath plasma. This large separation in the direction perpendicular to the magnetosheath flow suggests that the ionospheric plasma in the clouds must have originated in the ionosphere upstream on the dayside, indicating that MHD instabilities may occur at the Venusian ionopause. Therefore, Elphic and Ershkovich (1984) analyzed the stability of the Venusian ionopause by using one-fluid MHD equations for a perfectly conducting, incompressible, inviscid fluid, and concluded that the Kelvin–Helmholtz instability is the dominant instability over most of the dayside ionopause. After that, the Venusian solar wind–ionosphere interaction was analyzed using analytical (e.g., Elphic and Ershkovich, 1984) and numerical models (e.g., Thomas and Winske, 1991). Recently, Terada et al. (2002) used a global hybrid simulation to describe the Kelvin–Helmholtz instability at Venus.

Elphic and Ershkovich (1984) mentioned that under certain circumstances, the interchange instability can also develop at the Venusian ionopause. The interchange instability is similar in nature to the Rayleigh–Taylor instability in classic hydrodynamics, where the magnetic tension plays the role of an effective gravitational force (Chandrasekhar, 1961). In space plasmas, there exist structures, which have thin, curved boundary layers separating magnetic fields and plasmas of different origin. Magnetospheres of planets and magnetic clouds are typical examples of such structures. The interchange instability was proposed as an important process occurring at the Earth’s magnetopause (Rezhenov and Maltsev, 1994). Recently, Arshukova et al. (2004) showed that the Venusian ionopause can also be subject to the interchange instability.

## **2 Plasma behavior in the Venusian magnetosheath**

Even though a planet is unmagnetized, the flow of the solar wind is strongly affected by the interplanetary magnetic field (IMF). This interaction is studied by using a number of MHD approaches, used in a terrestrial context as well as for other planetary environments (e.g., Zwan and Wolf, 1976; Biernat et al., 1999). Studying the terrestrial magnetosheath, Zwan and Wolf (1976), Erkaev (1988), and others, predicted the presence of a region adjacent to the sunward side of the magnetopause where the influence of the magnetic field is very strong. In this so-called “magnetic barrier”, the magnetic field increases, while remaining finite, and simultaneously the plasma density decreases there, thus, this

region is also named “plasma depletion layer”. As a consequence, the plasma beta is below unity in this region.

Considering a steady-state situation, we model the plasma in a planetary magnetosheath as a nondissipative fluid which obeys the standard ideal MHD equations (in cgs units) (e.g., Weitzner, 1983) extended for mass loading processes

$$\begin{aligned} \nabla \cdot \left[ \rho \mathbf{U} \mathbf{U} + \Pi \mathbf{I} - \frac{1}{4\pi} \mathbf{B} \mathbf{B} \right] &= 0, \\ \nabla \cdot (\rho \mathbf{U}) &= N_0 m_0 s, \\ \nabla \cdot \mathbf{B} &= 0, \\ \nabla \times (\mathbf{U} \times \mathbf{B}) &= 0, \\ \nabla \cdot \left\{ \left[ \frac{1}{2} \rho U^2 + \frac{\kappa}{\kappa - 1} p \right] \mathbf{U} + \frac{1}{4\pi} \mathbf{B} \times (\mathbf{U} \times \mathbf{B}) \right\} &= 0. \end{aligned} \quad (1)$$

In (1),  $\Pi$  is the sum of the gas and magnetic pressures,  $\Pi = p + B^2/8\pi$ , while quantity  $\rho$  is the mass density.  $\mathbf{B}$  and  $\mathbf{U}$  are the magnetic field and plasma flow velocity, respectively. The parameter  $\kappa$  denotes the ratio of specific heats ( $\kappa = 5/3$ ), and  $\mathbf{I}$  is the unit dyadic. In descending order, we have the momentum and mass conservation equations, the condition that the magnetic field is divergence-free, the induction equation of the magnetic field for an infinitely conducting fluid, and the energy conservation equation.  $N_0$  and  $m_0$  are the density and mass of neutral particles, respectively, while  $s$  is the ion production rate.

An important feature of the problem is that the solar wind flow upstream of the planetary bow shock is generally supersonic and superalfvénic, so that

$$p_\infty \ll \rho_\infty U_\infty^2, \quad \text{and} \quad B_\infty^2 \ll 4\pi \rho_\infty U_\infty^2. \quad (2)$$

A consequence of these conditions is the existence of a detached shock separating the upstream interplanetary medium (denoted by  $\infty$ , and assumed uniform) from the magnetosheath. Across the shock the “Rankine–Hugoniot” jump relations must be satisfied (Biernat et al., 1999). There are corresponding boundary conditions at the ionopause. We model this boundary as a tangential discontinuity satisfying

$$U_n = 0, \quad \text{and} \quad B_n = 0. \quad (3)$$

We work with the following dimensionless variables

$$\begin{aligned} \mathbf{R}' &= \frac{\mathbf{R}}{R_0}, \\ p' &= \frac{p}{\rho_\infty u_\infty^2}, \\ \mathbf{B}' &= \frac{\mathbf{B}}{B_\infty}, \\ \mathbf{U}' &= \frac{\mathbf{U}}{U_\infty}, \end{aligned} \quad (4)$$

where  $\mathbf{R}$  is the position vector  $(x, y, z)$ , and  $R_0$  is the curvature radius of the ionopause at the subsolar point. Further, we introduce a parameter  $\varepsilon$ , depending on the upstream

quantities as

$$\varepsilon = \frac{B_\infty^2}{4\pi\rho_\infty U_\infty^2}. \quad (5)$$

This parameter is the inverse square of the Alfvén Mach number  $M_{A\infty}$ . Using the dimensionless set of variables, we transform the initial system of MHD equations (1) into the following set of equations,

$$\begin{aligned} \rho(\mathbf{U} \cdot \nabla)\mathbf{U} + \nabla\Pi &= \varepsilon(\mathbf{B} \cdot \nabla)\mathbf{B} - q(\mathbf{R})\mathbf{U}, \\ \nabla \cdot (\rho\mathbf{U}) &= q(\mathbf{R}), \\ \nabla \cdot \mathbf{B} &= 0, \\ \nabla \times (\mathbf{U} \times \mathbf{B}) &= 0, \\ \nabla \cdot \left\{ \left[ \frac{1}{2}\rho U^2 + \frac{\kappa}{\kappa-1}p \right] \mathbf{U} + \varepsilon \mathbf{B} \times (\mathbf{U} \times \mathbf{B}) \right\} &= 0, \end{aligned} \quad (6)$$

with  $\Pi = p + \varepsilon B^2/2$ . Here  $q(\mathbf{R})$  is a normalized ion source function,

$$q(\mathbf{R}) = q_0 \exp\left(\frac{R_0 - R}{H_0}\right),$$

with  $q_0 = N_0 m_0 s R_0 / (\rho_\infty U_\infty)$ , and  $H_0$  is the scale height of oxygen. We use a typical value for the mass loading parameter of  $q_0 \sim 1$ . We use the model shape of the ionopause which is a composite surface made up of a hemispherical surface (of radius  $R_0$ ) on the sunward side smoothly attached to a surface of revolution on the nightside, given by

$$x = \begin{cases} 1.4 - 1.3r^4, & r \geq 0.98 \\ \sqrt{1 - r^2}, & r \leq 0.98, \end{cases} \quad (7)$$

where  $r = \sqrt{y^2 + z^2}$ . Our ionopause flares out slightly on the nightside by an amount which decreases as we go further tailwards.

We integrate the MHD equations after bringing them to a special form, called ‘‘string equations’’ (see details in Biernat et al., 1999). The numerical scheme is based on the Lax-Wendroff method. We use a simplifying assumption concerning the behavior of the total pressure  $\Pi$ . In our method, its variation along the ionopause surface obeys the well-known Newtonian formula. For the total pressure variations along the normal to the obstacle we use the quadratic approximation

$$\Pi = \Pi_m \left(1 - \frac{\mu^2}{\delta^2}\right) + \Pi_s \frac{\mu^2}{\delta^2}, \quad (8)$$

where  $\mu$  is the distance from the ionopause along any given normal, and  $\Pi_m$  and  $\Pi_s$  are the values of the total pressures at the ionopause, and just downstream of the bow shock (with  $\Pi_m > \Pi_s$ ), respectively, and  $\delta$  is the distance from the ionopause to the bow shock along the normal. Quantity  $\Pi_s$  satisfies the jump conditions at the bow shock. For the variation of  $\Pi_m$  along the ionopause, we have

$$\Pi_m = (\Pi_0 - \Pi_\infty) \cos^2 \theta + \Pi_\infty. \quad (9)$$

In this expression,  $\Pi_0$  is the total pressure on the ionopause at the stagnation point of the flow, and  $\theta$  is the angle between the radius vector to a given point on the obstacle and the stagnation streamline. However, the solution is not very sensitive to the precise variation of the total pressure as this quantity is the one which varies least in the (computed) magnetosheath and depletion layer.

In Figure 1, from top to bottom, the first two panels show variations of the mass density and the total velocity along different stream lines (1–10) at the ionospheric boundary. The corresponding stream lines are shown at the bottom panels. Each stream line starts from the stagnation line and goes along the ionopause. The stream line number 10 corresponds to the ionopause in the  $XY$ -plane for  $Z = 0$ . The dashed line shows the shape of the obstacle in the  $XZ$ -plane at  $Y = 0$ . One can see in Figure 1, that the highest plasma flow velocities appear at the flanks near the equatorial plane, where the velocity reaches about  $0.8 U_\infty$ . This results from the fact that magnetic forces destroy the axial symmetry of the plasma flow around the ionosphere. The plasma flow is accelerated at the flanks in direction perpendicular to the magnetic field lines. This acceleration is caused by strong magnetic field tension in the magnetic barrier. Near the terminator, the velocity is only about  $0.2 U_\infty$  and near the subsolar point, the velocity tends to zero, indicating that this region is stable against the Kelvin-Helmholtz instability, as also pointed out by Elphic and Ershkovich (1984). The plasma density reaches values of about  $3.5 n_\infty$  near the subsolar point, while it decreases to  $1.5 n_\infty$  at the terminator and at the flanks in the equatorial plane.

### 3 The Interchange Instability at Venus

The equilibrium of the subsolar ionopause is provided by pressure balance, namely, the ionosphere plasma pressure is equal to the solar wind dynamic pressure. The plasma pressure has a specific non-monotonic behavior from the bow shock towards the ionosphere: First it decreases to a minimal value in the magnetic barrier and then it increases again to a large value corresponding to the ionosphere. This is the case when the interchange instability has to grow up. This instability is similar in nature to the Rayleigh–Taylor instability in classical hydrodynamics (Chandrasekhar, 1961), where the magnetic stress plays the role of an effective gravitational force. The interchange instability modes grow up when the magnetic tension acts in direction of the gradient of the plasma pressure in the layer.

To describe non-steady variations of the magnetic field and plasma parameters we use the ideal MHD equations (Arshukova et al, 2004). We shall use the two coordinates  $y$  and  $z$  as the distances along the geodetic lines on the surface with equal curvature radii  $R$ . The third coordinate  $x$  is the distance along the normal to the surface. We assume that the density of plasma is not constant, but  $\nabla \cdot \mathbf{U} = 0$ . This simplification is reasonable, because the interchange perturbations are developing much slower than the magnetosonic waves propagate (see details in Arshukova et al., 2004). For computational convenience, we introduce the dimensionless parameters

$$\tilde{x} = x/R_0, \quad \tilde{\mathbf{k}} = \mathbf{k}R_0,$$

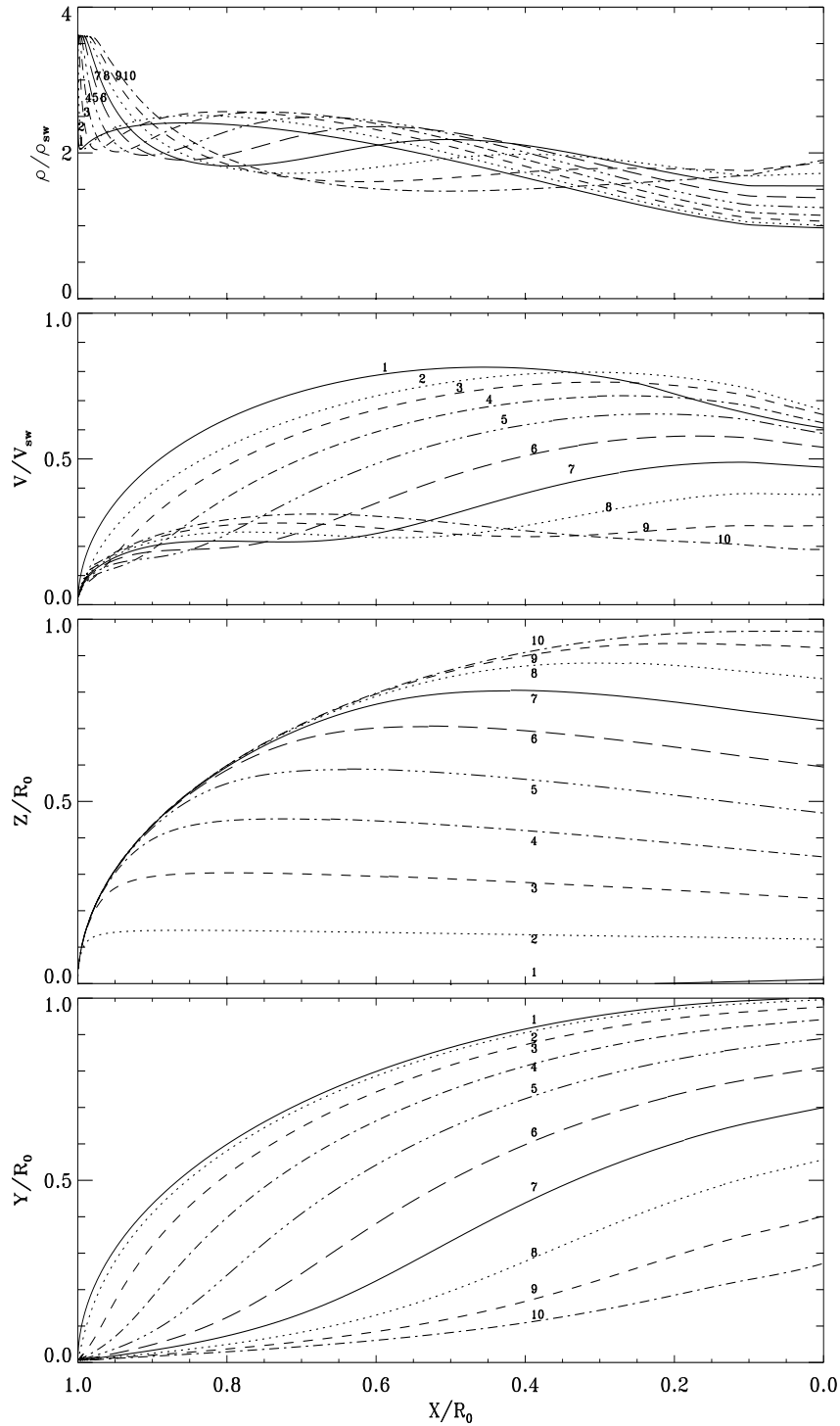


Figure 1: From top to bottom: The first panel is the mass density variations along different stream lines near the ionopause; the second panel is the total velocity variation along different stream lines; the last two panels show the stream lines along the ionopause. The third panel shows the stream lines in the  $XZ$ -plane coplanar to the IMF, while the fourth panel gives stream lines in the  $YZ$ -plane perpendicular to the IMF.

$$\begin{aligned}
\tilde{\rho} &= \rho/\rho_\infty, & \tilde{\omega} &= \omega R_0/U_\infty, \\
\tilde{t} &= tU_\infty/R_0, & \tilde{\mathbf{B}} &= \frac{\mathbf{B}}{\sqrt{4\pi\rho_\infty U_\infty^2}}, \\
\tilde{\mathbf{U}} &= \mathbf{U}/U_\infty, & \tilde{\Pi} &= \frac{\Pi}{\rho_\infty U_\infty^2}.
\end{aligned} \tag{10}$$

Furthermore, we introduce small perturbations of the magnetic field and the plasma parameters,

$$\mathbf{B} = \mathbf{B}^* + \mathbf{b}, \quad \mathbf{U} = \mathbf{U}^* + \mathbf{u}, \quad \Pi = \Pi^* + \Pi', \quad \rho = \rho^* + \rho',$$

where  $|\mathbf{b}| \ll |\mathbf{B}|$ ,  $|\mathbf{u}| \ll |\mathbf{U}|$ ,  $\Pi' \ll \Pi$ ,  $\rho' \ll \rho$ . Small perturbations of the magnetic field, velocity and plasma pressure are treated in a linear approximation. We consider all perturbations to be proportional to the complex exponential function  $\exp(i(\mathbf{k} \cdot \mathbf{s} - \tilde{\omega}t))$ , where  $\mathbf{s}$  is a two-dimensional vector in the plane  $(y, z)$ . Finally, we obtain a second order linear ordinary differential equation for the Fourier amplitude of the total pressure perturbation  $\tilde{\Pi}$  depending on the  $x$  coordinate. Regarding the boundary conditions, we assume the instability disturbances to vanish in the ionosphere and in the solar wind region upstream of the bow shock. As a background, we use the profiles of the magnetic field and plasma parameters along the subsolar line which are obtained from our numerical MHD flow model for mass loading parameter  $q_0 = 1$ .

Figure 2 shows the normalized interchange instability growth rate as a function of the dimensionless parameter  $kR_0$  for typical values of the magnetic field and plasma density (Arshukova et al., 2004). The different curves 1, 2, 3, 4, 5, 6, 7 correspond to different ion densities of the ionosphere normalized to the solar wind density,  $\tilde{\rho}_i = 10, 20, 50, 100, 200, 300, 500$ , respectively. This instability growth rate is a monotonic increasing function of the wave number. Perturbations with small length scales are the most unstable ones. In the figure, the maximal parameter  $kR_0 \sim 50$  corresponds to the length scale  $\lambda \sim k^{-1} \sim R_0/50 \sim 130$  km. The instability is weaker for larger ion densities in the ionosphere.

The physical value of the growth rate  $\gamma^*$  can be found by multiplication of the dimensionless quantity by the normalization factor

$$\gamma^* = \gamma U_\infty / R_0.$$

From Figure 2 one can find that the maximum dimensionless growth rate corresponding to  $kR_0 \sim 50$  exceeds the ratio  $U_\infty/R_0$ . And correspondingly, the instability growth time  $\tau^*$  defined as  $1/\gamma^*$  is less than  $R/U_\infty$ . It is important to compare the instability growth time with the time scale  $\tau_m$  of the magnetic barrier formation, which can be estimated as the time of the transport of a frozen-in magnetic field line from the bow shock to the ionopause. This time scale is given by an integral along the subsolar line from the bow shock to the stagnation point,

$$\tau_m = - \int_{1+\delta_p}^{X_s} \frac{1}{U_x} dX.$$

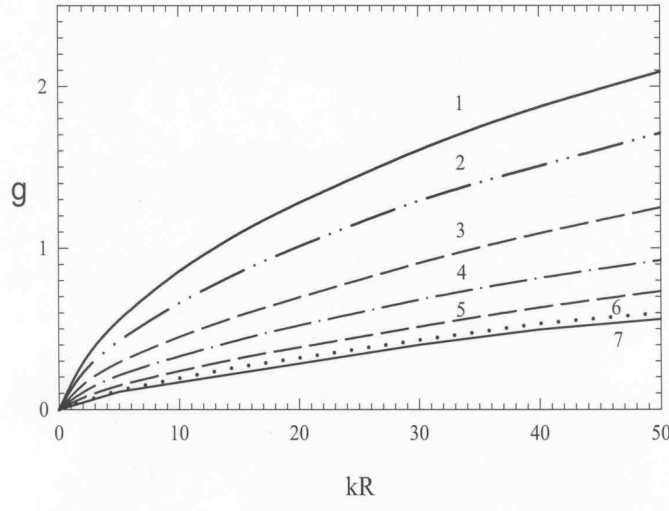


Figure 2: Growth rate of the interchange instability as a function of the wave number for different normalized ionospheric plasma densities; curves (1, 2, 3, 4, 5, 6, 7) correspond to  $\tilde{\rho}_i = (10, 20, 50, 100, 200, 300, 500)$ , respectively.

Taking a simple linear approximation for the velocity along the stagnation stream line  $U_x = -U_s(X - 1)/\Delta_s$ , we find

$$\tau_m = \frac{\Delta_s}{U_s} \ln(\Delta_s/\delta_p).$$

Here  $\Delta_s$  and  $U_s$  are the magnetosheath thickness and the velocity just downstream of the shock, respectively. Quantity  $\delta_p$  is a small length scale where the frozen-in condition is not valid because of kinetic plasma effects. We consider this distance  $\delta_p$  to be equal to the ion plasma scale which is about 100 km. For Venus we find  $\Delta_s \sim 0.27R_0$  and  $U_s = (\rho_\infty/\rho_s)U_\infty \sim U_\infty/3.3$ . Taking  $R = 6400$  km, we obtain finally the estimation  $\tau_m \sim 2.6 R_0/U_\infty$ . Therefore, the instability growth time is less than that of the magnetic barrier formation.

Figure 3 shows the distribution of the total pressure as function of the  $x, y$  coordinates for  $\tilde{\rho}_i = 10$ , and  $kR_0 = 30$ . From this figure one can see that the perturbations are mainly localized within the magnetic barrier. They do not disturb the magnetosheath region adjacent to the bow shock. The interchange instability can bring about an enhanced diffusion of magnetic field in vicinity of the dayside ionopause.

## 4 The Kelvin–Helmholtz instability at Venus

Another instability, which can appear at the Venusian ionopause, is the Kelvin–Helmholtz instability. This instability arises from a shear velocity between two separated plasma regions, with the well-known example that the air flowing above a sea surface causes surface waves in the sea.

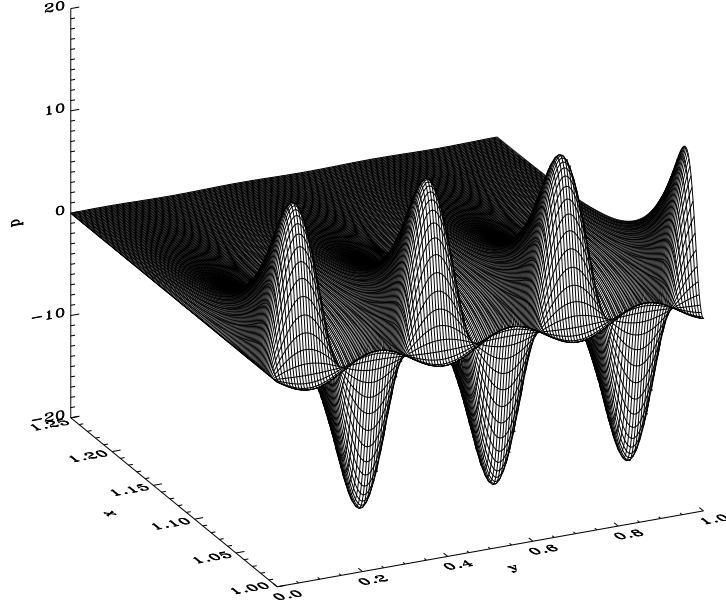


Figure 3: Distribution of the total pressure perturbations as a function of the  $(x, y)$  coordinates.

The Pioneer Venus Orbiter mission showed that the solar wind interaction takes place with the ionosphere/atmosphere system at Venus. Therefore, the shear velocity between the magnetosheath and the ionospheric plasma leads to the appearance of the Kelvin–Helmholtz instability in certain regions of the Venusian ionopause. Different aspects of this interaction were analyzed by several authors during the last 20 years (Wolff et al., 1980; Elphic and Ershkovich, 1984; Terada et al., 2002). To describe the Kelvin–Helmholtz instability, it is not appropriate to use an ideal MHD description, because for this case the shortest wavelength would give the largest instability growth rates, the so-called “zero wavelength anomaly” (Wolff et al., 1980). To achieve a realistic result, it is necessary to include two effects, the influence of gravity (Chandrasekhar, 1961; Elphic and Ershkovich, 1984) and the finite Larmor radius effect causing the viscous interaction between the two plasma regions (Wolff et al., 1980).

We use the MHD equations derived by Wolff et al. (1980) including gravity and the finite Larmor radius effect. After some algebra (Wolff et al., 1980), the dispersion relation is found to be

$$\omega = k \frac{\rho_1 U_1 + \rho_2 U_2}{\rho_1 + \rho_2} + k |k| \frac{\nu_2 \rho_2 - \nu_1 \rho_1}{\rho_1 + \rho_2} \pm i \left( k^2 \frac{\rho_1 \rho_2 (U_2 - U_1)^2}{(\rho_1 + \rho_2)^2} + 2 \left| k^3 \frac{(\nu_1 + \nu_2) \rho_1 \rho_2 (U_2 - U_1)}{(\rho_1 + \rho_2)^2} - k^4 \left( \frac{\nu_2 \rho_2 - \nu_1 \rho_1}{\rho_1 + \rho_2} \right)^2 - |k| \frac{g(\rho_2 - \rho_1)}{\rho_1 + \rho_2} \right)^{1/2} \right). \quad (11)$$

Here,  $\nu$  represent the viscous coefficient, and subscripts 1 and 2 denote magnetosheath and ionosphere conditions, respectively. The expression under the root represents the instability growth rate. If this expression is positive, disturbances of the interface exist with an amplitude growing with time. Therefore, the surface becomes unstable. It is obvious that the first term under the radical in equation (11) is always positive. This term

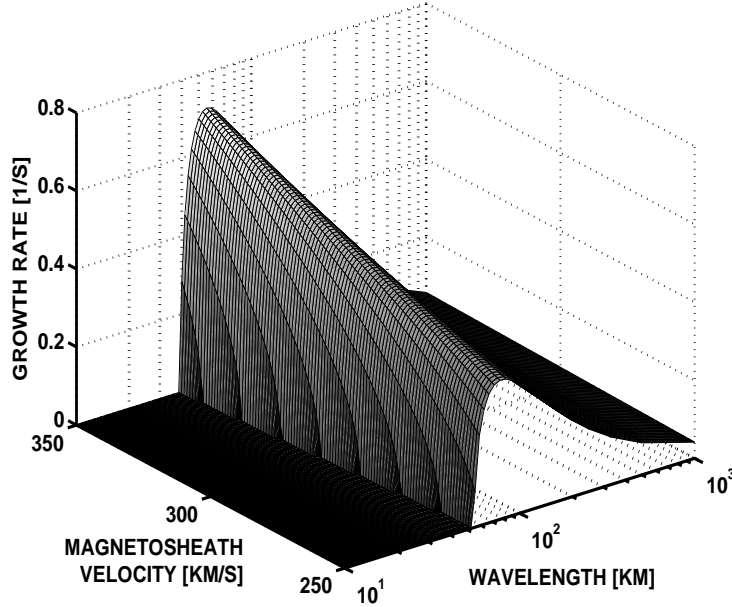


Figure 4: Instability growth rate as a function of the magnetosheath velocity and the wavelength.

corresponds to the Kelvin–Helmholtz instability in ideal MHD, and tends to destabilize the surface. The second and the third terms arise from the viscous interaction, and are relevant for short wavelength stabilisation (Terada et al., 2002). The fourth term describes the stabilisation due to gravity, which is important for the long wavelength stabilisation. The quantities necessary to evaluate the instability growth rates can be achieved from measurements as well as from model calculations. To describe the conditions in the Venusian magnetosheath, we use the model presented in the previous chapters. For the ion number density and composition, we use the study of (Nagy et al., 1980), while the ionospheric velocities derived by (Knudsen, 1992) are used.

Using these quantities, we are able to calculate the instability growth rates occurring in different regions of the Venusian ionopause. Near the subsolar point the shear velocity between the magnetosheath and the ionosphere is small, therefore this region is stable against the Kelvin–Helmholtz instability, as proposed by different studies (Wolff et al., 1980; Elphic and Ershkovich, 1984). At the polar terminator, the shear flow is larger, therefore the instability growth rates in this region are smaller than the magnetic barrier formation time (see previous section). If we use the velocity distribution from the previous chapters (see also Penz et al., 2004, 2005), we find that the flow velocities at the equatorial flanks near the terminator plane are the largest. For this region, we achieve instability growth rates, which are nearly one order-of-magnitude larger than at the polar terminator (Figure 4). Since this region was not investigated in the study of Brace et al. (1982), it is possible to achieve much larger escape rates, if we assume that most of the escape takes place at the equatorial flanks. Therefore, the Kelvin–Helmholtz instability is an important ion loss process occurring at Venus.

## 5 Conclusions

Based on an MHD model for the solar wind flow past Venus, the growth times for MHD instabilities are calculated. We found that both, the interchange instability and the Kelvin–Helmholtz instability, have growth times smaller than the characteristic time scales of the system. The interchange instability most likely arises near the subsolar point. The largest growth rates for the Kelvin–Helmholtz instability are found at the equatorial flanks, followed by the polar terminator region. It is unlikely that the Kelvin–Helmholtz instability occurs near the subsolar point. Our results indicate that the instabilities can evolve into a non–linear stage, giving rise to detached plasma clouds. This is an important non–thermal loss process at Venus.

## Acknowledgements

This work is supported by the Austrian “Fonds zur Förderung der wissenschaftlichen Forschung” under project P17099–N08, by project Nr. I.2/04 from “Österreichischer Austauschdienst”, and by grants 04–05–64088 and 03–05–20014 BNTS a from the Russian Foundation of Basic Research. Also acknowledged is support by the “Verwaltungsstelle für Auslandsbeziehungen” of the Austrian Academy of Sciences.

## References

- Arshukova, I. L., N. V. Erkaev, H. K. Biernat, and D. F. Vogl, Interchange instability of the Venusian ionopause, *Adv. Space Res.*, **33**, 182, 2004.
- Bauer, S. J., *Physics of Planetary Ionospheres*, Springer–Verlag, New York–Heidelberg–Berlin, 1973.
- Biernat, H. K., N. V. Erkaev, and C. J. Farrugia, Aspects of MHD flow about Venus, *J. Geophys. Res.*, **104**, 12617, 1999.
- Biernat, H. K., N. V. Erkaev, and C. J. Farrugia, MHD effects in the Venus magnetosheath including mass loading, *Adv. Space Res.*, **28**, 833, 2001.
- Brace, L. H., R. F. Theis, and W. R. Hoegy, Plasma clouds above the ionopause of Venus and their implications, *Planet. Space Sci.*, **30**, 29, 1982.
- Chandrasekhar, S., *Hydrodynamic and hydromagnetic stability*, Oxford Univ. Press, New York, 1961.
- Elphic, R. C., and A. I. Ershkovich, On the stability of the ionopause of Venus, *J. Geophys. Res.*, **89**, 997, 1984.
- Erkaev, N. V., Results of the investigation of MHD flow around the magnetosphere (review), *Geomag. Aeron.*, **28**, 455, 1988.

- Erkaev, N. V., C. J. Farrugia, and H. K. Biernat, Effects on the Jovian magnetosheath arising from solar wind flow around non-axisymmetric bodies, *J. Geophys. Res.*, **101**, 10665, 1996.
- Farrugia, C. J., N. V. Erkaev, H. K. Biernat, and L. F. Burlaga, Anomalous magnetosheath properties during Earth passage of an interplanetary magnetic cloud, *J. Geophys. Res.*, **100**, 19245, 1995.
- Kallio, E., J. G. Luhmann, and J. G. Lyon, Magnetic field near Venus: A comparison between Pioneer Venus Orbiter magnetic field observations and an MHD simulation, *J. Geophys. Res.*, **103**, 4723, 1998.
- Knudsen, W. C., The Venus ionosphere from in situ measurements, in *Venus and Mars: Atmospheres, Ionospheres, and solar wind interaction*, J. G. Luhmann, M. Tatallyay, and R. O. Pepin (Eds.), Geophysical Monograph 66, American Geophysical Union, Washington, USA, 1992.
- Nagy, A. F., T. E. Cravens, S. G. Smith, H. A. Taylor, and H. C. Brinton, Model calculations of the dayside ionosphere of Venus: Ionic composition, *J. Geophys. Res.*, **85**, 7795, 1980.
- Penz, T., N. V. Erkaev, H. K. Biernat, H. Lammer, U. V. Amerstorfer, H. Gunell, E. Kallio, S. Barabash, S. Orsini, A. Milillo, and W. Baumjohann, Ion loss on Mars caused by the Kelvin–Helmholtz instability, *Planet. Space Sci.*, **52**, 1157, 2004.
- Penz, T., I. L. Arshukova, N. Terada, H. Shinagawa, N. V. Erkaev, H. K. Biernat, and H. Lammer, A comparison of magnetohydrodynamic instabilities at the Martian ionopause, *Adv. Space Res.*, in press, 2005.
- Rezhenov, B. V., and Y. P. Maltsev, Role of interchange instability in flux transfer event origin, *Ann. Geophys.*, **12**, 183, 1994.
- Terada, N., S. Machida, and H. Shinagawa, Global hybrid simulation of the Kelvin–Helmholtz instability at the Venus ionopause, *J. Geophys. Res.*, **107**, 1471, 2002.
- Thomas, V. A., and D. Winske, Kinetic simulation of the Kelvin–Helmholtz instability at the Venus ionopause, *Geophys. Res. Lett.*, **18**, 1943, 1991.
- Weitzner, H., Linear wave propagation in ideal magnetohydrodynamics, in *Handbook of Plasma Physics*, Vol. 1, A. A. Galeev, and R. N. Sudan (Eds.), North–Holland, New York, 201, 1983.
- Wolff, R. S., B. E. Goldstein, and C. M. Yeates, The onset and development of Kelvin–Helmholtz instability at the Venusian ionopause, *J. Geophys. Res.*, **85**, 7697, 1980.
- Zwan, B. J., and R. A. Wolf, Depletion of the solar wind plasma near a planetary boundary, *J. Geophys. Res.*, **81**, 1636, 1976.